Electronic Supplementary Information (ESI)

Sol-gel synthesized, low-temperature processed, reduced molybdenum peroxides for organic optoelectronics applications

A. M. Douvas,[*a] *M. Vasilopoulou,*[a] *D. G. Georgiadou,*[a] *A. Soultati,*[a,b] *D. Davazoglou,* [a] *N. Vourdas,*[a] *K. P. Giannakopoulos,*[a] *A. G. Kontos,*[a] *S. Kennou,*[c] *and P. Argitis*[a]

[a] *Institute of Nanoscience and Nanotechnology (INN), National Center for Scientific Research "Demokritos", 15310 Aghia Paraskevi, Athens, Greece*

[b] *Department of Chemical Engineering, National Technical University of Athens, 15780 Athens, Greece*

[c] *Department of Chemical Engineering, University of Patras, 26504 Patra, Greece*

[*] Correspondence to: Dr. A. M. Douvas. E-mail: adouvas@imel.demokritos.gr

1. UV-Vis monitoring of ox/red Mo peroxides in solution. Analogous observations with the thermal reactions of ox/red Mo peroxide films have been also made in

solution (Fig. S1). In particular, the thermal reduction of the ox-Mo peroxide in the precursor solution at 170 °C proceeds also through the reduction/destruction of the peroxo group, which is initially significantly blue-shifted in solution (316 nm; Fig. S1a). The difference

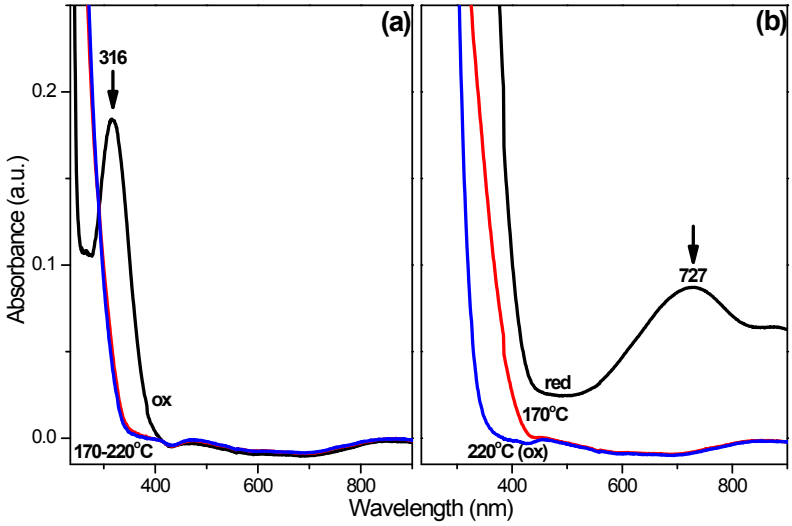

Figure S1. UV-Vis monitoring of: (a) thermal reduction of ox-Mo peroxide, and (b) thermal reoxidation of red-Mo peroxide, both in solution containing H_2O_2 upon heating from RT to 220 °C.

in that case is that no IVCT band appears during the thermal reduction of the ox-Mo peroxide in solution, possibly because of the excess of H_2O_2 in solution, which rapidly reoxidizes the thermally reduced Mo peroxide.

On the other hand, the thermal reoxidation of a red-Mo peroxide in solution proceeds exactly with the same way as in films, i.e. with the disappearance of the IVCT band upon heating at 170 °C (Fig. S1b). In this case, the initial Mo peroxide was reduced in solution through the synthesis route presenting an IVCT band at 727 nm. The thermal reoxidation of the red-Mo peroxide in solution (at 170 °C) is much more effective than in films (where heating at least at 200 °C is needed) due to the presence of H_2O_2

in solution. The inability of reformation of peroxo group in solution containing excess of H_2O_2 during the thermal reoxidation of a red-Mo peroxide indicates that the reduction of the peroxo group in solution is irreversible.

2. FT-IR changes in water content during thermal treatment of ox/red Mo peroxide films. Initially, an ox-Mo peroxide film presents a broad absorption band at ~3421 cm^{-1} and a weak band at 1649 cm^{-1} ascribed to stretching and bending vibration of OH groups (ν, δ(OH) respectively) of coordinated water molecules (Fig. S2a, b). Also, a weak peak

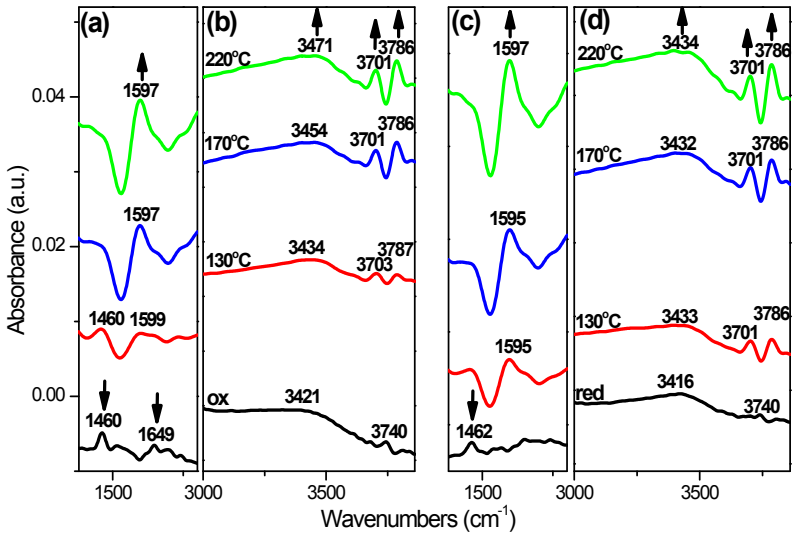

Figure S2. FT-IR changes in water content of: (a, b) an oxidized Mo peroxide film, and (c, d) a solution-reduced Mo peroxide film, upon annealing from RT to 220 °C.

at 1460 cm^{-1} attributed to bending of Mo−OH group of adsorbed water molecules is shown.[1-6] Thus, coordinated water molecules are mainly present in the initial ox-Mo peroxide film, whereas a small percentage of adsorbed water molecules also coexists. Heating of the ox-Mo peroxide film (especially at a high temperature, $T \geq 170$ °C; Fig. S2a, b) causes increase in intensity of both ν(OH) and δ(OH) bands of coordinated water molecules (accompanied by a shift to higher and lower energy, i.e.

at 3471 and 1597 cm^{-1}, respectively), whereas the weak δ(OH) band at 1460 cm^{-1} vanishes. Those changes indicate that upon high temperature ($T \geq 170$ °C) thermal treatment of an ox-Mo peroxide film, the number of coordinated water molecules increases, whereas the adsorbed water molecules completely vanish, a finding which is in accordance with literature for WO_3 films.[3,4] Furthermore, it is noteworthy that except for the increase of the broad ν(OH) band (at 3471 cm^{-1}) upon high temperature heating, two sharp ν(OH) peaks at higher wavenumbers (i.e. at 3701 and 3786 cm^{-1}) also increase in intensity. The broad ν(OH) band could be attributed to water molecules bound by both hydrogens to the MoO_3 lattice, whereas the two sharp ν(OH) peaks at higher wavenumbers could be ascribed to water molecules bound by the oxygen to the lattice.[2] Analogous observations are also made during the thermal treatment of a solution-reduced Mo peroxide film (Fig. S2c, d).

3. FT-IR changes during thermal treatment of a solution-reduced Mo peroxide film. During thermal treatment of a solution-reduced Mo peroxide film the following infrared changes (see text, Fig. 3) are observed: (a) progressive decrease of PEG bands (2930, 2875, and 1123 cm^{-1}, where only a weak broad band at 1076 cm^{-1} remains) up to 220 °C indicating that PEG is gradually removed upon annealing of the solution-reduced Mo peroxide film. (b) Complete vanishing of the weak peroxo band at 917 cm^{-1} indicating that the remaining peroxo groups are thermally reduced. (c) Progressive formation of a single Mo═O band with intermediate position at 967 cm^{-1} (from the two initial Mo=O bands) and gradual increase of two bands at 563 and 680 cm^{-1} attributed to Mo−O−Mo bridges. The latter changes indicate possible structural modification in the coordination of Mo ions as previously mentioned.

4. Raman study of ox/red Mo peroxide films. Similar to the FT-IR results obtained during thermal treatment of ox/red Mo peroxide films were also taken with Raman spectroscopy (Fig. S3). Micro-Raman spectra of Mo peroxide films were obtained on silicon wafers with Renishaw inVia Reflex microscope using an Ar^+ ion laser (at 514.5 nm) as excitation source. The laser beam was focused onto the samples by means of a 50x objective and the laser power density was 0.4 mW μm^{-2}.

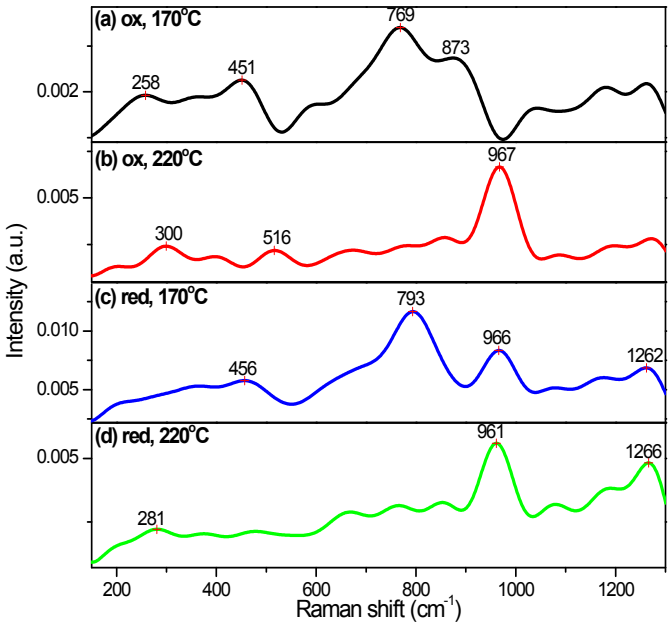

Figure S3. Raman changes during thermal treatment of: (a, b) an oxidized Mo peroxide film, and (c, d) a solution-reduced Mo peroxide film. The films were heated at: (a, c) 170 °C, and (b, d) 220 °C.

In particular, when an ox-Mo peroxide film was annealed at 170 °C two broad bands at 873 and 769 cm^{-1} were mainly observed. The band at 873 cm^{-1} can be attributed to both stretching modes of ν(Mo═O) and ν(−O−O−), whereas the band at 769 cm^{-1} to ν(Mo−O−Mo). There is also a broad band at 451 cm^{-1} that could be attributed to deformation δ(Mo−O−Mo) with a small contribution of ν(Mo−O_2).[7-10] Upon further heating of the ox-Mo peroxide film at 220 °C, the peroxo band at 873 cm^{-1} and the

v(Mo−O−Mo) peak at 769 cm^{-1} vanish and a new peak at 967 cm^{-1} attributed only to *v*(Mo═O) emerges. On the other hand, a (solution) reduced Mo peroxide film heated at 170 °C presents three main bands: at 966 cm^{-1} attributed to *v*(Mo═O), at 793 cm^{-1} attributed to *v*(Mo−O−Mo) with a small contribution of *v*(−O−O−), and at 456 cm^{-1} attributed to *δ*(Mo−O−Mo) with a small contribution of *v*(Mo−O_2). Upon further heating of the red-Mo peroxide film at 220 °C, the band at 793 cm^{-1} disappears and only the band at 961 cm^{-1} ascribed to *v*(Mo═O) remains. From the above it is evident that upon thermal treatment of both ox/red Mo peroxide films up to 220 °C, the peroxo groups and possibly some Mo−O−Mo bridges are cleaved, whereas at the end of heating (at 220 °C) of both films a MoO_3 film is possibly formed, since similar spectra were obtained.

5. XRD characterization of ox/red Mo peroxide films. The crystal structure of ox/red Mo peroxide films at different temperatures was investigated with x-ray diffraction (XRD, Fig. S4). Wide angle X-ray diffraction analysis was carried out in reflection mode using a Bruker D8 Discover diffractometer with Ni-filtered Cu-Kα radiation (λ = 1.5406 Å) equipped with a LynxEye position sensitive detector. In particular, upon thermal treatment of an ox-Mo peroxide film, the film changes from an amorphous phase with a low percentage of orthorhombic MoO_3 (*o*-MoO_3) at 150 and 220 °C to a complete *o*-MoO_3 at 500 °C with the characteristic crystalline planes [002], [102], and [171].[11,12] On the other hand, a solution-reduced Mo peroxide film heated at 220 °C shows a characteristic diffraction peak ascribed to [011] plane of H_xMoO_3 along with the characteristic peak attributed to [171] plane of *o*-MoO_3 indicating that it is a mixture of H_xMoO_3 and *o*-MoO_3.[11,13]

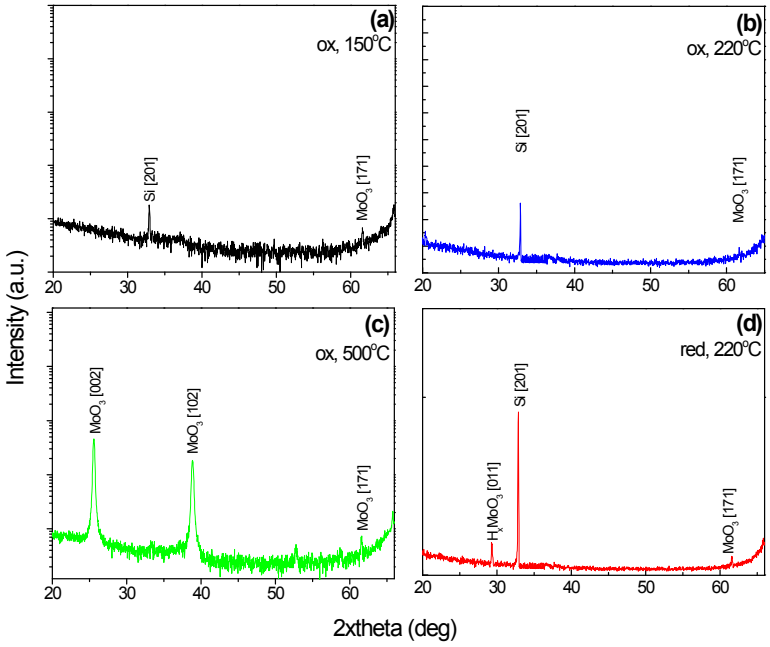

Figure S4. XRD pattern evolution during thermal treatment of an ox-Mo peroxide film at: (a) 150 °C, (b) 220 °C, and (c) 500 °C. (d) XRD pattern of a solution-reduced Mo peroxide film thermally treated at 220 °C.

6. Optical characterization of ox/red Mo peroxide films with spectroscopic ellipsometry. The change of refractive index and extinction coefficient (*n*, *k*) with wavelength and thickness measurements during thermal treatment of ox/red Mo peroxide films was investigated with spectroscopic ellipsometry (Fig. S5). Spectroscopic ellipsometry measurements of Mo peroxide films were conducted on a J. A. Woollam Inc. M2000F rotating compensator ellipsometer (RCE^{TM}) running the WVASE32 software at 75.14° incidence angle. In an ox-Mo peroxide film (a, b), it was proved that both *n*, *k* increase with temperature (*T*). Exactly the same was observed in a solution-reduced Mo peroxide film (c, d), where the increase of *n*, *k* was more abrupt at 220 °C. Also, from the relation of *n*, *k* with *T*, the change of film thickness with temperature was extracted (e, f).[14] It was observed that the decrease of film thickness with temperature was clearly more abrupt during thermal treatment

between 130 and 170 °C in ox-Mo peroxide films (e), possibly due to the thermal reduction/destruction of the peroxo group.

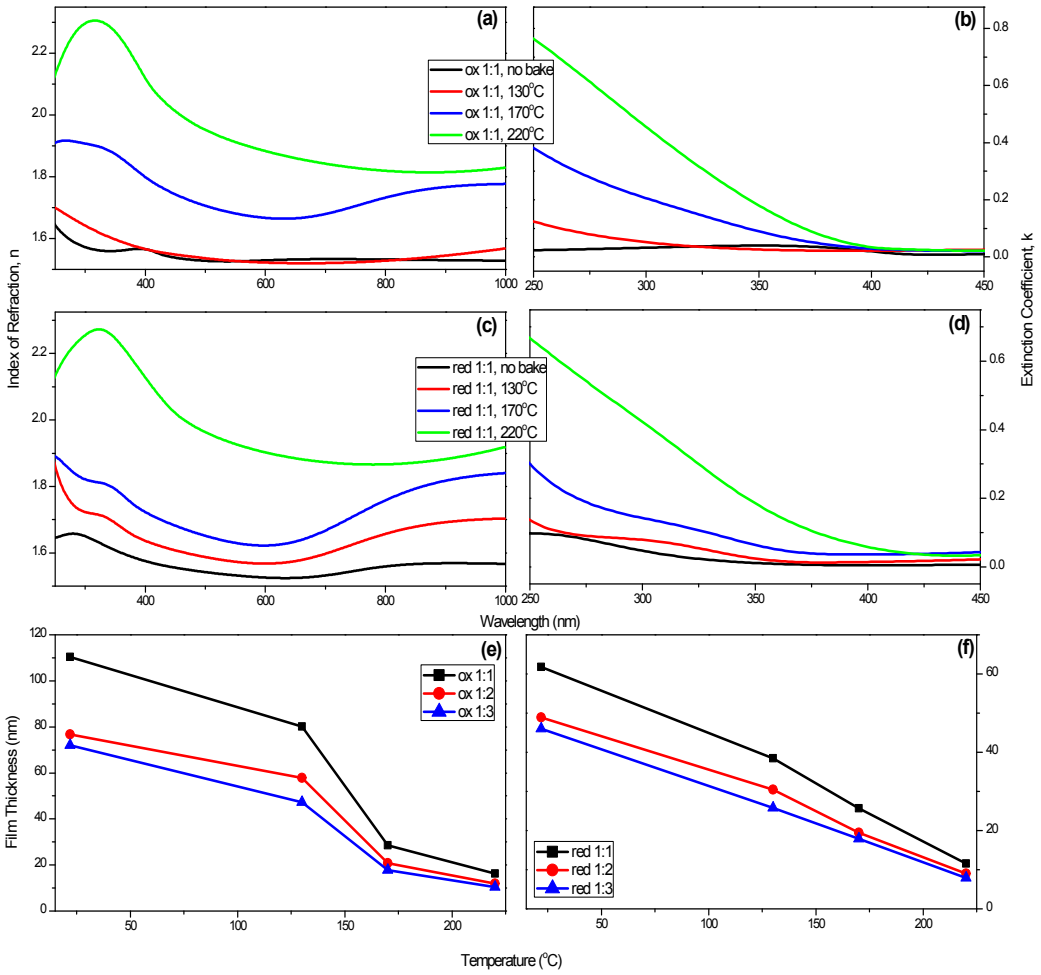

Figure S5. Change of refractive index (a) and extinction coefficient (b) with wavelength during thermal treatment of an oxidized Mo peroxide film. The same in a solution-reduced Mo peroxide film (c, d). Change of film thickness with annealing temperature of ox- and red- Mo peroxide films (e, f). The films were thermally treated from RT to 220 °C. (The ox/red Mo peroxide solutions were diluted with 2ME at a volume ratio ranging from 1:1 to 1:3, where in the reduced solutions the excess of H_2O_2 had been evaporated).

Also in (e), the inclination of the curve at that temperature range decreases with the increase of dilution with 2ME, a finding which is an indirect proof that upon increase of dilution with 2ME the reduction degree of Mo peroxide increases. On the other

hand in (f), when a (solution) reduced Mo peroxide was further diluted with 2ME, no abrupt decrease of film thickness at that temperature range (130-170 ^{o}C) was observed, obviously because the majority of peroxo groups had been initially reduced.

7. Morphological characterization of ox/red Mo peroxide films with SEM/TEM. For the surface and bulk characterization of the molybdenum peroxide films, a LEO Supra 35 VP scanning electron microscope (SEM) and a PHILLIPS CM20 transmission electron microscope (TEM) were used. The morphological characterization of ox/red Mo peroxide films is very important, as the morphology is considered to significantly affect the device performance. In the present work, the effect of reduction of Mo peroxide films either through the solution synthesis route or the thermal treatment of films on the morphology of Mo peroxide films was mainly studied. It is proved -from the SEM characterization- that upon increase of annealing temperature of an ox-Mo peroxide film from 150 to 500 ^{o}C (Fig. S6a-d), the grain size increases (e.g. the grain size almost doubles going from 360 to 500 ^{o}C). Nevertheless, the most important point is the significant improvement of film morphology upon reduction through the synthesis route. In particular, the surface homogeneity of a red-Mo peroxide film considerably increases in comparison with an ox-Mo peroxide film thermally treated at the same temperature (220 ^{o}C; Fig. S6e, f). That surface homogeneity enhancement possibly contributed decisively in the improvement of the device performance.

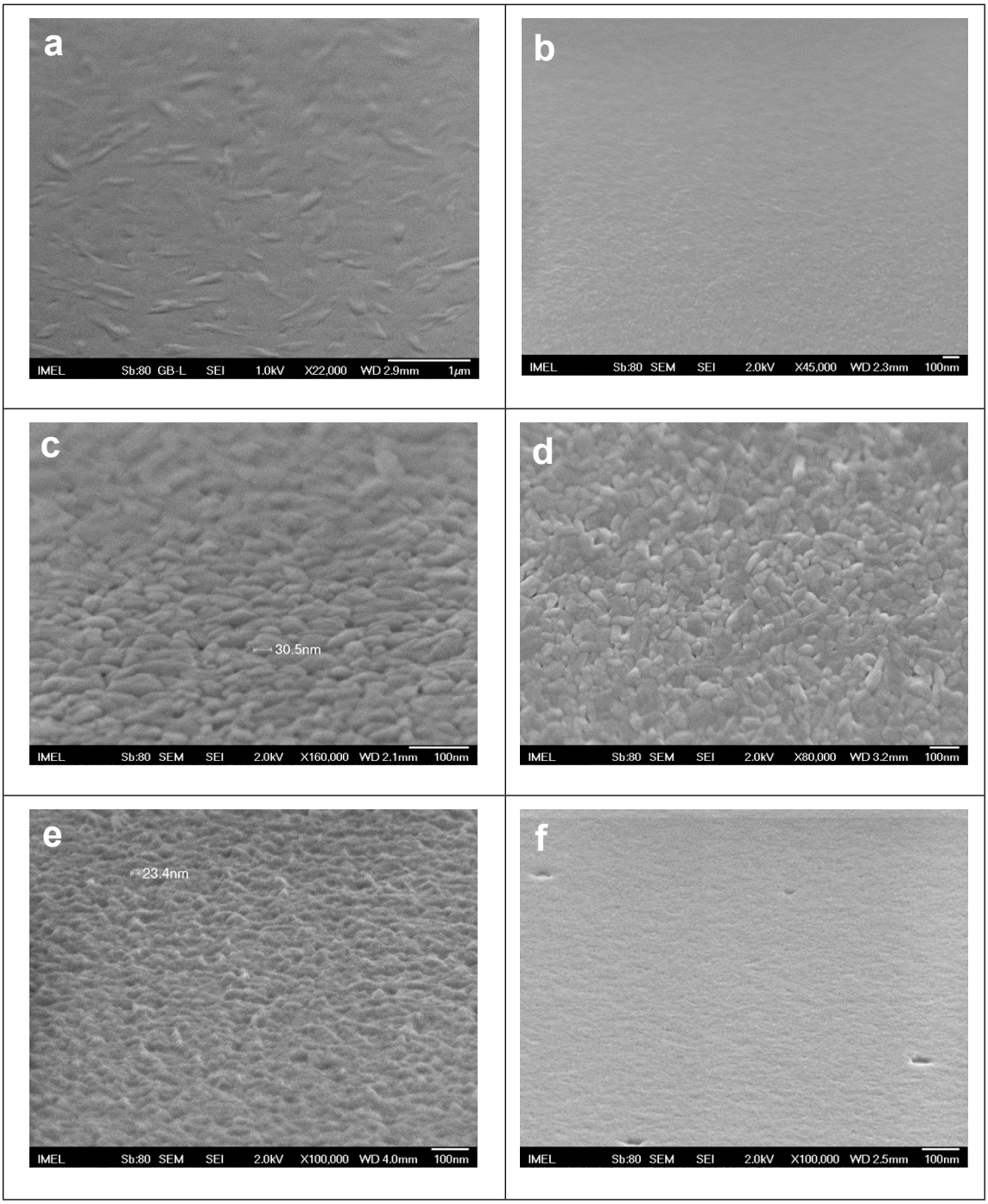

Figure S6. SEM images of an ox-Mo peroxide film thermally treated at different temperatures: (a) 150 ^{o}C, (b) 250 ^{o}C, (c) 360 ^{o}C, and (d) 500 ^{o}C. Also, SEM images of: (e) an ox- and (f) a red-Mo peroxide film thermally treated at 220 ^{o}C (where the precursor solution was diluted 1:1 v/v with 2ME). Film thickness in: (a) 196 nm, (d) 37.5 nm, (e) 33 nm, (f) 30 nm).

On the other hand, from the TEM characterization of the films it is shown that the ox-Mo peroxide films (Fig. S7a, b) are fiber-like, where the coverage of the fibers consists mainly of PEG and the core of the fibers consists of Mo according to EDAX examination.

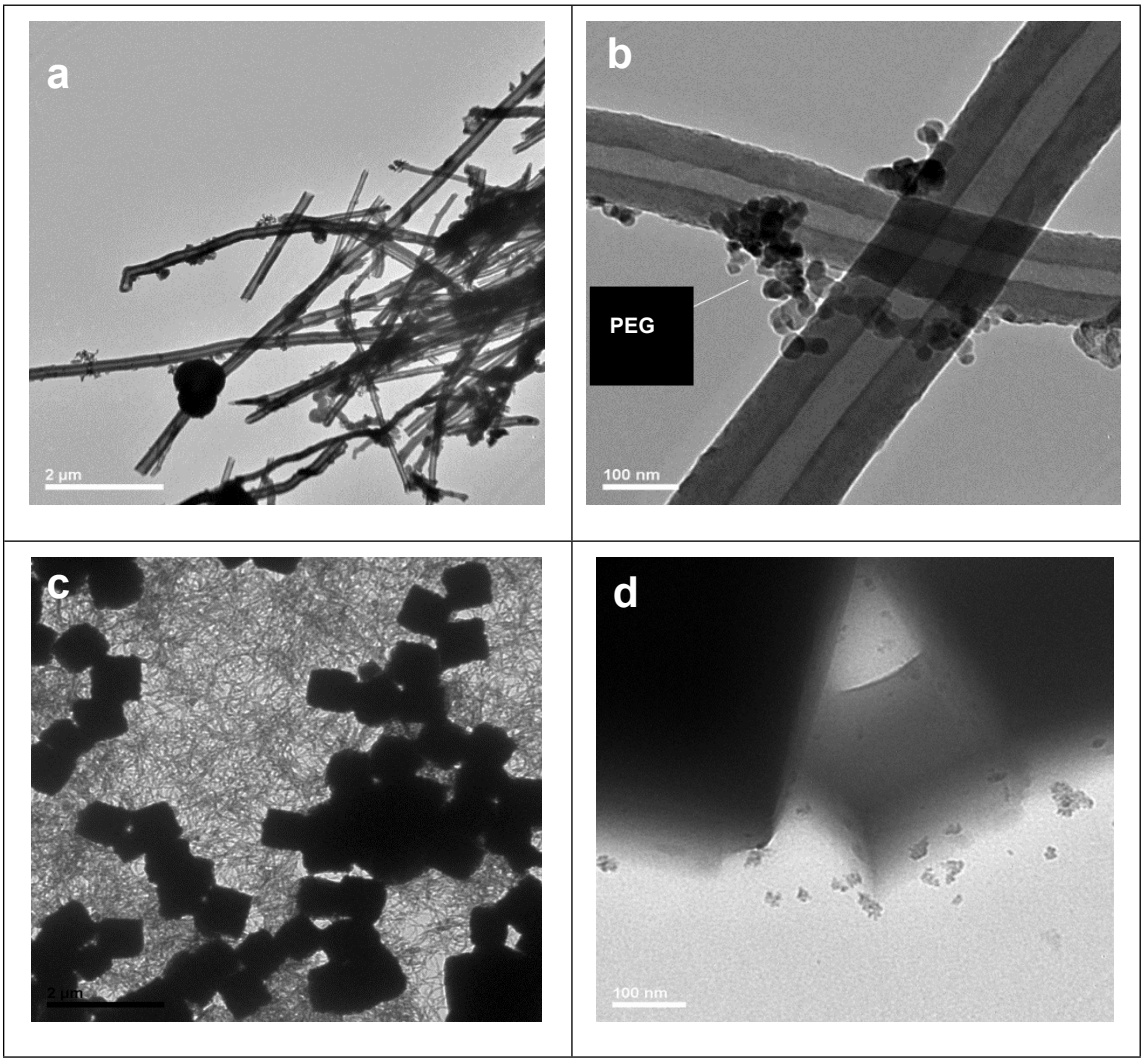

Figure S7. TEM images (in low magnification, 2500-8200) of: (a, b) an ox- and (c, d) a red-Mo peroxide film. (The precursor solutions of both Mo peroxides were diluted 1:3 v/v with 2ME, where in the reduced solution the excess of H_2O_2 had been removed).

In contrast, it is noteworthy that the red-Mo peroxide films (Fig. S7c, d) are cubic-like, where onto the cubes a high concentration of Mo was detected, whereas outside of the cubes there was a high concentration of C attributed to PEG. Thus, it is

apparent that upon reduction through the modified synthesis route nanoparticles of Mo peroxide form that improve significantly the homogeneity of the films.

References

1 K. Segawa, K. Ooga, Y. Kurusu, *Bull. Chem. Soc. Jpn.,* 1984, **57**, 2721.

2 S. E. Horsley, D. V. Nowell, D. T. Stewart, *Spectrochimica Acta,* 1974, **30A**, 535; L. Bertsch, H. W. Habgood, *J. Phys. Chem.,* 1963, **67**, 1621.

3 M. F. Daniel, B. Desbat, J. C. Lassegues, B. Gerand, M. Figlarz, *J. Solid State Chem.,* 1987, **67**, 235.

4 M. F. Daniel, B. Desbat, J. C. Lassegues, R. Garie, *J. Solid State Chem.,* 1988, **73**, 127.

5 N. Mizuno, K. Katamura, Y. Yoneda, M. Misono, *J. Catal.,* 1983, **83**, 384.

6 K. Eguchi, Y. Toyozawa, N. Yamazoe, T. Seiyama, *J. Catal.,* 1983, **83**, 32.

7 M. K. Chaudhuri, N. S. Islam *Transition Met. Chem.,* 1985, **10**, 333.

8 K. Yamanaka, H. Oakamoto, H. Kidou, T. Kudo, *Jpn. J. Appl. Phys.,* 1986, **25**, 1420.

9 L. Seguin, M. Figlarz, R. Cavagnat, J.-C. Lassègues, *Spectrochimica Acta A,* 1995, **51**, 1323.

10 K. Eda, *J. Solid State Chem.,* 1992, **98**, 350.

11 A. Soultati, A. M. Douvas, D. G. Georgiadou, L.C. Palilis, J. M. Feckl, S. Gardelis, M. Fakis, S. Kennou, P. Falaras, T. Stergiopoulos, D. Davazoglou, P. Argitis, M. Vasilopoulou, *Adv. Energy Mater.,* 2014**,** **4**, DOI: 10.1002/aenm.201300896.

12 S.-Y. Lin, C.-M. Wang, K.-S. Kao, Y.-C. Chen, C.-C. Liu, *J. Sol-Gel Sci. Technol.,* 2010, **53**, 51.

13 R. Murugan, A. Ghule, C. Bhongale, H. Chang, *J. Mater. Chem.,* 2000, **10**, 2157.

14 G. Papadimitropoulos, N. Vourdas, K. Giannakopoulos, M. Vasilopoulou, D. Davazoglou, *J. Appl. Phys.,* 2011, **109**, 103527.